Neural Comput & Applic (2019) 31:3187–3200
DOI 10.1007/s00521-017-3263-6

ORIGINAL ARTICLE

EEG-based tonic cold pain recognition system using wavelet transform

Rami Alazrai[1] · Mohammad Momani[2] · Hussein Abu Khudair[3] · Mohammad I. Daoud[1]

Received: 22 September 2016 / Accepted: 14 October 2017 / Published online: 30 October 2017

Abstract Developing an objective pain identification system can provide caregivers with a second opinion to improve the treatment of patients who are unable to verbally communicate their pain. In this study, we present a new EEG-based approach for pain recognition. The proposed approach is employed to identify four different states that a human can feel during tonic cold pain stimulation. These states are the relax state, relax-to-pain state (RPS), pain state (PS), and pain-to-relax state (PRS). A sliding window has been used to decompose the EEG signals into overlapping segments. Each EEG segment is analyzed using the discrete wavelet transform to construct a time–frequency representation of the EEG signals and extract a set of nonlinear features. These features are used to construct a two-layer hierarchical classification framework that can identify the aforementioned four pain states. The first layer identifies whether an EEG segment is relax or pain segment. In the second layer, the pain segments are classified into one of the three pain states (i.e., RPS, PS, and PRS). To evaluate the performance of the proposed approach, we recorded EEG data for 24 healthy subjects who were exposed to tonic cold pain stimulation. Three procedures were employed to evaluate the capability of the approach to detect the four states associated with tonic cold pain stimulation. The experimental results demonstrate the efficacy of our approach for accurate tonic cold pain identification. Moreover, these promising results suggest the feasibility of expanding the proposed approach to characterize clinical pain, such as cancer-related pain.

Keywords Tonic cold pain recognition · Electroencephalogram (EEG) · Higher-order statistics (HOS) · Discrete wavelet transform (DWT) · Hierarchical classification · Support vector machines (SVM)

1 Introduction

Pain is a complex unpleasant experience that is conveyed to the brain when sensory neurons are stimulated by a potential injury or illness [31]. The subjective nature of pain perception increases the difficulty to measure and quantify the intensity of pain [10, 20]. Toward this end, several subjective-based approaches have been explored for clinical pain assessment, such as visual analogue scale (VAS), verbal rating scale (VRS), and numerical rating scale (NRS) [39]. These pain assessment approaches require the intervention of caregivers in order to determine the pain intensity of the patient using interview-based procedure. Despite the fact that the subjective-based pain assessment approaches are widely used for clinical pain assessment, these approaches are inadequate for individuals who are unable to verbally communicate their pain, such as infants and unconscious patients [18]. Therefore, objective pain characterization is considered highly desirable for clinical pain assessment and management.

The recent advancements in noninvasive neuroimaging techniques, such as functional magnetic resonance imaging

✉ Rami Alazrai
rami.azrai@gju.edu.jo

[1] Department of Computer Engineering, School of Electrical Engineering and Information Technology, German Jordanian University, Amman 11180, Jordan

[2] Department of Communication Engineering, School of Electrical Engineering and Information Technology, German Jordanian University, Amman 11180, Jordan

[3] Department of Anesthesiology and Pain Management, King Hussein Cancer Center (KHCC), Amman 11941, Jordan

(fMRI), electroencephalography (EEG), and positron emission tomography (PET), have facilitated the investigation of stimulated human pain using various types of exogenous noxious stimuli. These neuroimaging techniques have enabled the identification of several cortical regions in the brain that are involved in the pain perception mechanism [19, 31, 37]. Among the different neuroimaging techniques, EEG is considered the most commonly used neuroimaging modality. This can be attributed to several factors such as the high temporal resolution, relative low cost, and high portability [25].

Recently, researchers have investigated the use of EEG signals to monitor the changes in brain activities in order to detect pain. For example, Panavaranan and Wongsawat [28] conducted a study to detect acute thermal pain in human using power spectral density (PSD)-based features that are extracted from the EEG signals. EEG data were collected from nine healthy subjects, and pain was stimulated using a thermal pad. Using the extracted features, a support vector machine (SVM) classifier was used to classify the EEG signals into two different states: rest and pain. In addition, a fuzzy logic system was used to estimate the level of the acute thermal pain. Nir et al. [27] investigated the use of peak alpha frequency (PAF) as an objective measure associated with subjective perception of tonic heat pain. EEG signals were acquired from 18 healthy subjects, and heat tonic pain was stimulated through a thermal contact-heat simulator. Experiments showed that the relevance of PAF to the neural processing of tonic pain may produce some useful features to characterize pain. Nevertheless, the brain perception mechanism of tonic pain stimulation is still considered an active research area. This is due to the high induced effect of tonic pain compared to other painful stimuli such as impairments in visual task performance and memory performance [22, 34]. Furthermore, several studies have shown that clinical pain can be simulated using tonic pain in a way better than the other types of pain stimuli [9, 27]. In this vein, Rissacher et al. [32] conducted a study to detect tonic cold pain in human using frequency-based features extracted from EEG signals. EEG data were collected from 15 healthy subjects, and pain was stimulated by immersing the participant's left hand in ice water. Experimental results showed that the temporal-parietal decrease in alpha frequency band during pain can be a useful feature for pain assessment. In another study, Vatankhah and Toliyat [38] utilized wavelet coherency in order to estimate three different tonic cold pain levels: no-pain, pain, and unbearable pain. Furthermore, in order to identify the three pain levels in EEG signals, discrete wavelet transform was used to extract first-order and second-order statistical features. Then, the extracted features were utilized to build two different classifiers, namely SVM and hidden Markov model (HMM) classifier. Experimental results showed that using SVM with RBF kernel has achieved a better classification accuracies compared with HMM. Shao et al. [33] performed a frequency-domain EEG source analysis in order investigate the electrocortical brain responses to tonic cold pain. EEG signals were acquired from 26 healthy subjects under two different states related to tonic cold pain stimulation, namely pain and no-pain states. Experiments showed that the cortical power changes between different frequency bands in various brain regions can be utilized to characterize the perception of tonic cold pain.

In the aforementioned approaches, tonic cold pain was analyzed by considering only the frequency domain of EEG signals, such as the power spectrum and the coherence values. This kind of analysis neglects the nonstationarity nature of EEG signals as well as the time-varying characteristics of pain in the acquired EEG signals [4, 36]. Furthermore, the previous approaches have not taken into consideration the nonlinear interactions between EEG components. These nonlinear characteristics of EEG signals are highly related to the underlying pain perception mechanisms [35]. Recently, researchers have started to use higher-order statistics to model the nonlinear interactions in EEG signals. For example, Hadjileontiadis [17] proposed an approach that combined continuous wavelet transform (CWT) with higher-order statistics (HOS) in order to characterize tonic cold pain in EEG signals. The proposed approach was evaluated using EEG data that were collected from 17 healthy subjects, and the results were promising in terms of discriminating between rest and pain states.

In this paper, a feasibility study is presented to investigate the use of EEG signals analysis based on discrete wavelet transform for recognizing tonic cold pain. In particular, our proposed approach aims to identify four different tonic cold pain states that a subject can feel during tonic cold pain stimulation. The first state is the no-pain or the relax state (RS). During this state, the subject is relaxing and feeling no pain. The second state represents the transition from the relax state to mild pain. We denote this state as the relax-to-pain state (RPS). During this state, the subject starts to feel a mild pain due to the applied tonic cold pain stimulus. Applying the tonic cold pain stimulus for a longer period of time increases the pain feeling from mild to severe pain. We denote the state in which the subject is feeling severe pain as the pain state (PS). Finally, the fourth state represents the transition from the pain state to the relax state. We denote this state as the pain-to-relax state (PRS). During this state, the subject starts to feel that

the pain is reducing due to the absence of the tonic cold pain stimulus. In order to identify the aforementioned four different states from EEG signals, a sliding window is employed to decompose the EEG signals into overlapping segments. Then, we utilize discrete wavelet transform (DWT) to provide a time–frequency representation of the EEG segments which can describe the dynamic changes in the EEG signals during tonic pain stimulation. Using the time–frequency representation, we extract a set of nonlinear features, including two HOS-based features (skewness and kurtosis), autoregressive coefficients, entropy, and energy. Combining both the time–frequency representation and the extracted nonlinear features enables to provide a dynamic identification of nonlinearities across different EEG signals. Using the extracted nonlinear features, we construct a hierarchical classification framework that can identify the four different tonic cold pain states. Specifically, the hierarchical classification framework consists of two layers. In the first layer, we utilize the nonlinear features extracted from EEG segments to train a binary SVM classifier to discriminate EEG segments that comprise any of the three pain states (i.e., RPS, PS, and PRS) from EEG segments that do not comprise pain. This layer can be viewed as a spotting stage that can identify whether an EEG segment contains pain feeling or not. The EEG segments that are classified as a potential pain segments are passed on to the second classification layer. In the second layer, we train a SVM classifier to identify the three different states associated with tonic cold pain intensity, namely RPS, PS, and PRS.

In order to evaluate the proposed approach, we have recorded EEG data for 24 healthy subjects who were exposed to tonic cold pain stimulation. Then, three different performance evaluation procedures are developed to evaluate the performance of the proposed approach in identifying the four different tonic cold pain states using the EEG signals. The three performance evaluation procedures are: wavelet-based performance evaluation procedure, channel-based performance evaluation procedure, and frequency band-based performance evaluation procedure. These three evaluation procedures quantify the effect of the utilized wavelet function, EEG channel location, and EEG frequency band on the capability of the proposed approach to characterize tonic cold pain states.

The remainder of this paper is organized as follows: In Sect. 2, we describe the procedure employed to collect the EEG-based tonic cold pain data, the proposed wavelet-based nonlinear features, the classification model, and the evaluation procedures. Experimental results and discussion are presented in Sect. 3. Finally, the conclusion and future directions are provided in Sect. 4.

2 Materials and methods

2.1 Subjects

In this study, twenty-four right-handed healthy subjects (11 females and 13 males) volunteered to participate in the experiments. The mean ± standard deviation age of the subjects was 23.5 ± 2.3 years. Furthermore, the subjects were non-smokers, not taking any prescribed medication related to neurological or psychiatric problems, and not experiencing any pain prior to the acquisition of the EEG signals. The experimental procedure, which is described in Sect. 2.2, was explained in detail for each subject, and a signed consent form was collected from each subject before participating in the experiment. Furthermore, the participants had the chance to withdraw from the study at anytime during the experimental procedure. The study was reviewed and approved by the institutional review board (IRB) at the German Jordanian University.

2.2 Experimental procedure

In this study, we have adopted an experimental procedure that is similar to the experimental procedures employed in several previous studies, such as [17, 32, 33, 38]. Specifically, each subject was seated on a comfortable upright chair at a distance of approximately 0.5 meter from a laptop displaying a black image on its screen. The laboratory used in the tonic cold pain stimulations had a controlled temperature of 24–26 °C, attenuated sound conditions, and faint lighting.

All subjects participated in the experiments with their eyes open. Each subject was instructed to keep his/her right hand relaxed on a table located in front of him/her for approximately 30 s. This period represents the relax state (RS). Then, each subject was instructed to submerge his/her right hand in a bucket of iced water with a temperature of 1.5 ± 2.5 °C and use his/her left hand to click the mouse button of the laptop to indicate the end of the RS and the start of the relax-to-pain state (RPS). When the subject started to have a moderate uncomfortable feeling, he/she performed a second mouse-click using the left hand to indicate the end of the PRS and the start of the pain state (PS). Thereafter, the subject is persistent to submerge his/her hand in the bucket of iced water until the pain became unbearable, and at that moment he/she removed his/her right hand from the bucket and performed a third mouse-click to indicate the end of the PS. Finally, when the subject started to feel that the pain has reduced and reached to a moderate stage, he/she performed a fourth mouse-click. The period between the third and fourth mouse-clicks represents the pain-to-relax state (PRS). The fourth mouse-

click marks the end of one experiment trail. For each subject, the experimental procedure was repeated for four additional times. In order to guarantee that the subject starts the trials from the relax state (i.e., the no-pain condition), each subject was asked after the fourth mouse-click to submerge his/her right hand in a bucket of warm water with a temperature of $40 \pm 1\,^{\circ}\mathrm{C}$ and count down for three seconds starting from a random 4-digit number until he/she reached the relax state [14].

2.3 EEG data acquisition and preprocessing

The EEG data were recorded using the Emotiv EPOC + hi-resolution 14-channel wireless EEG Neuroheadset (http://www.emotiv.com). The Emotiv EPOC + system employs the international 10–20 EEG system to localize 14 hi-resolution channels at the following locations: AF3, AF4, F3, F4, F7, F8, FC5, FC6, O1, O2, P7, P8, T7, and T8, referenced to the CMS and DRL at locations P3 and P4, respectively [15]. The Emotive EPOC + system acquires EEG signals internally at a sampling frequency of 2048 Hz. The acquired EEG signals are filtered using a hardware band-pass filter with a bandwidth of 0.2–43 Hz. Furthermore, the Emotiv EPOC + applies two digital notch filters at 50 and 60 Hz. Finally, EEG signals are down sampled to 128 samples per second. In order to remove the strong muscle artifacts, we have applied the procedure that was used in [33]. Specifically, we have visually inspected the EEG signals and manually removed the distorted EEG segments. In addition, EEGlab [13] was utilized to remove eye-movement/blinking artifacts using the automatic artifact rejection (AAR) toolbox [16]. The mean $\pm$ standard deviation of the lengths of the recorded trials across all subjects is 8450 ± 1214 samples.

2.4 Time–frequency analysis of the EEG data

In this section, we describe the time–frequency analysis that has been applied to the acquired EEG signals. Furthermore, we provide a detailed description of the extracted nonlinear features. For the purpose of feature extraction, the signal of each EEG channel was processed using a sliding window of size $W = 128$ samples and overlap size of $O = 64$ samples. Then, for each channel, we applied a time–frequency transformation, namely the discrete wavelet transform (DWT). Using the obtained DWT coefficients, we calculate a set of nonlinear features at each window position. The DWT along with the set of nonlinear features extracted from the EEG signals is described in the next subsections.

2.4.1 Discrete wavelet transform (DWT)

Wavelet transform is a time–frequency representation in which a signal is represented as a linear combination of a collection of wavelet functions [3]. These wavelet functions are a scaled and translated versions of a particular function, which is usually called the mother wavelet. The ability of the wavelet transform to provide an optimal resolution in both time and the frequency domains makes it more suitable for representing non-stationary signals, such as EEG signals [1]. In addition, wavelet transform enables adequate description of an input signal by generating a limited number of coefficients called the wavelet coefficients. These coefficients measure the similarity between the signal and the wavelet functions. In this work, we used the DWT to analyze the EEG signals in the time–frequency domain and generate a set of features that can be used to characterize tonic cold pain in the acquired EEG signals.

DWT analyzes an input signal $x[n]$ at different frequency bands with different resolutions by decomposing the signal into coarse detail and approximation information. The detail coefficients are computed by filtering the input signal $x[n]$ using a high-pass filter ($h[\cdot]$) that represents a discrete mother wavelet. The approximation coefficients are obtained by filtering the signal using a low-pass filter ($g[\cdot]$). Then, the obtained filtered signals are down sampled by a factor of 2. To construct another level in the DWT decomposition structure, the down-sampled approximation coefficients are decomposed into a new set of detail and approximation coefficients. This procedure is repeated until the required number of decomposition levels is achieved. Figure 1 provides an illustration of the decomposition of a signal $x[n]$ into four different levels using DWT.

The analysis of the EEG signals using DWT is highly dependent on the number of decomposition levels and the selected wavelet function. In this work, the number of DWT decomposition levels is chosen in accordance with the number of EEG dominant frequency bands. Specifically, the number of decomposition levels is selected to be four. Table 1 shows the different EEG frequency bands along with the corresponding DWT decomposition levels. In order to determine the wavelet function, we have developed an evaluation procedure to quantify the effect of utilizing different wavelet functions on the accuracy of identifying different tonic cold pain states in the EEG signals as described in Sect. 2.6.

2.4.2 Feature extraction

Using the obtained DWT-based time–frequency representation, we extract a set of features from the computed detail and approximation coefficients. More specifically, at each

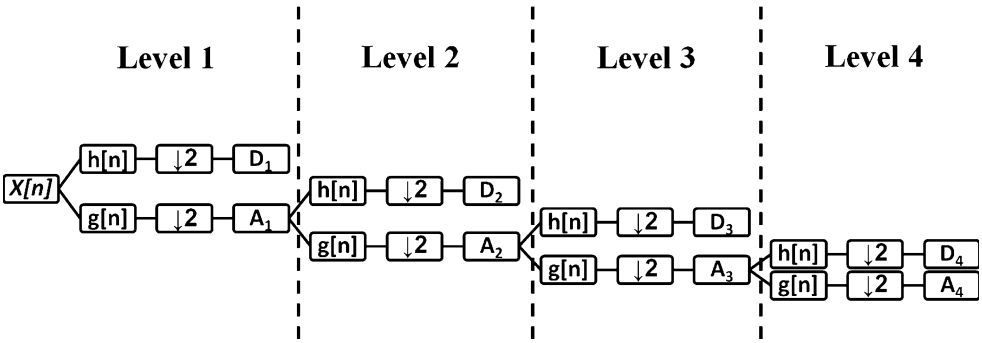

Fig. 1 Decomposition of the signal $x[n]$ into four levels using DWT. The notation $\downarrow 2$ represents the down sampling of the signal by a factor of two. D_i and A_i represent the detail and approximation coefficients, respectively, at level i

Table 1 Decomposing an EEG signal into five levels using DWT, where each level corresponds to a specific frequency band

Frequency band	Frequency range (Hz)	DWT decomposition level
Delta (δ)	0.2–4	A4
Theta (θ)	4–8	D4
Alpha (α)	8–13	D3
Beta (β)	13–30	D2
Gamma (γ)	30–43	D1

window position W, the DWT is applied to all EEG channels. Then, for each channel, four different types of nonlinear features are extracted from the obtained detail and approximation coefficients $(D_1, D_2, D_3, D_4, A_4)$. The extracted features are defined as follows:

1. *HOS-based features* The HOS-based features can quantify the nonlinear behavior of random processes such as EEG signals [26]. EEG signals are randomly distributed and involve nonlinear interactions between the different frequency components [12, 17]. Unlike first- and second-order statistics, using the HOS enables to characterize the nonlinear coupling and divergence from Gaussian behavior in the EEG signals. Furthermore, HOS are considered robust to Gaussian noise due to the fact that the values of HOS computed for Gaussian processes are statistically equal to zero [11]. Therefore, in this work, we utilize the DWT coefficients to compute two HOS features, namely the skewness and kurtosis. These two features can quantify the nonlinear changes in the EEG signals occurring during different tonic cold pain states. The skewness and kurtosis are defined as follows:

   A. *Skewness* is defined as the normalized third-order moment of a random variable with a specific probability distribution function. It measures the degree of asymmetry of a distribution around its mean [30]. The skewness indicates that a distribution is positively skewed, negatively skewed, or not skewed depending on whether the skewness value is positive, negative, or zero, respectively. The skewness is calculated for the DWT coefficients associated with the four different decomposition levels as follows:

$$S_C = \frac{\frac{1}{N}\sum_{i=1}^{N}(C(i)-\bar{C})^3}{\left(\sqrt{\frac{1}{N-1}\sum_{i=1}^{N}(C(i)-\bar{C})^2}\right)^3}, \quad (1)$$

   where $C \in \{D_1, D_2, D_3, D_4, A_4\}$, $C(i)$ is the i *th* element in the sub-band C, N is the number of DWT coefficients in C, and $\bar{C} = \frac{1}{N}\sum_{i=1}^{N} C(i)$ is the sample mean of the DWT coefficients in C .

   B. *Kurtosis* is defined as the normalized fourth-order moment of a random variable. The kurtosis value provides an indication of the tailedness of a distribution relative to the normal distribution [30]. In particular, a distribution with high kurtosis value indicates that the data are heavily tailed, which implies that the data contain outliers. On the other hand, a distribution with a small kurtosis value indicates that the data are light-tailed, which implies that the data include a relatively small number of outliers. The kurtosis is computed for the DWT coefficients associated with the four different decomposition levels as follows:

$$K_C = \frac{\frac{1}{N}\sum_{i=1}^{N}(C(i)-\bar{C})^4}{\left(\frac{1}{N}\sum_{i=1}^{N}(C(i)-\bar{C})\right)^2}. \quad (2)$$

2. *Autoregressive Coefficients-based features* The autoregressive (AR) model describes each sample of the obtained DWT coefficients as a linear combination of the previous samples along with a white noise error term [21, 23]. The AR model can be constructed as follows:

$$C(n) = \sum_{i=1}^{l} a_i C(n-i) + \varepsilon_n, \quad (3)$$

where a_i are the AR coefficients , ε_n represents white noise, and l represents the order of the AR model and is experimentally selected to be 4. In this work, the fourth-order AR coefficients are computed and used as features.

3. *Entropy* represents a statistical measure of the uncertainty of a signal. The entropy of the obtained DWT coefficients is computed as follows [24]:

$$\mathrm{ENT}_C = -\sum_{i=1}^{N}\Big(C(i)^2\log(C(i)^2)\Big). \tag{4}$$

4. *Energy* is computed by squaring the DWT coefficients associated with the four different decomposition levels as follows [24]:

$$\mathrm{ENG}_C = \sum_{i=1}^{N} C(i)^2. \tag{5}$$

Therefore, for a given DWT detail or approximation coefficients that are computed for the signal associated with an EEG channel at a specific window position, the number of extracted features is equal to eight, which include two HOS features, four AR coefficients, entropy, and energy. In the next section, we provide a detailed description of the proposed hierarchical classification framework for identifying the four different tonic cold pain states.

2.5 Classification of tonic cold pain states

Due to the subjective nature of pain feeling across different subjects, the number of samples associated with each of the four states associated with tonic cold pain stimulation can vary significantly. Therefore, this can lead to unbalance data samples across different classes, which in turn limits the direct application of multi-class SVM classifier to differentiate the four pain states considered in this study [5]. To address this limitation, we have proposed a hierarchical classification framework that consists of two layers: the relax/pain identification layer (Layer 1) and the pain state identification layer (Layer 2). The first layer identifies whether an EEG segment is relax or pain segment. In the second layer, the pain segments are classified into one of the three pain states (i.e., RPS, PS, and PRS). The input to the hierarchical classification framework is a set of nonlinear features extracted from an EEG segment bounded within a specific window position as depicted in Sect. 2.4.2. Figure 2 provides a schematic diagram of the proposed two-layer classification framework.

2.5.1 The relax/pain identification layer (Layer 1)

In this layer, we utilize the extracted nonlinear features to train a binary SVM classifier to recognize whether an EEG segment is a relax segment or a pain segment. More specifically, a relax segment is an EEG segment that belongs to the relax state (RS), whereas a pain segment is an EEG segment that belongs to one of the three pain states (i.e., RPS, PS, and PRS).

Using the binary SVM [8], the input data are mapped into a high-dimensional feature space by applying a kernel function. This mapping allows to compute a nonlinear decision function that can separate the feature space into two regions, one for each class. Specifically, consider a training set $\mathscr{D} = \{(\mathbf{X}_1, y_1), \ldots, (\mathbf{X}_k, y_k), \ldots, (\mathbf{X}_n, y_n)\}$, where $\mathbf{X}_k \in R^N$ represents a feature vector, and $y_k \in \{-1, +1\}$ represents the class of the vector $\mathbf{X}_k$. In particular, if y_k is equal to -1, then the EEG segment associated with the vector $\mathbf{X}_k$ contains no pain and represents the relax state (RS). Otherwise, the EEG segment associated with the vector $\mathbf{X}_k$ represents a pain segment. The goal of the binary SVM is to determine a decision function in the form of hyperplane that can separate the feature space into two regions through maximizing the margin between the samples of different classes. The resultant decision function is defined as follows:

$$f(\mathbf{X}) = \mathrm{sgn}\left(\sum_{i=1}^{n} y_i\alpha_i\varphi(\mathbf{X_i}, \mathbf{X}) + b\right), \tag{6}$$

where $\mathbf{X} \in R^N$ is a new feature vector to be classified into relax or pain, $\varphi(\mathbf{X_i}, \mathbf{X})$ is the kernel function that maps the input vectors into high-dimensional space, α_i is the i *th* Lagrange multiplier, y_i is the class of the sample $\mathbf{X_i}$, and b is the bias term of the decision hyperplane. Several kernel functions can be used with SVM. However, the Gaussian radial basis function (RBF) is the most commonly used kernel function for classification tasks. In this work, we utilize a RBF kernel with the SVM classifier. The RBF kernel function can be defined as follows:

$$\varphi(\mathbf{X_i}, \mathbf{X}) = \exp\left(-\frac{||\mathbf{X_i} - \mathbf{X}||^2}{2\sigma^2}\right), \tag{7}$$

where $\sigma > 0$ is the RBF kernel parameter.

After classifying the EEG segments into relax and pain classes, the EEG segments that are classified as pain segments are passed on to the pain state identification layer (Layer 2) to identify the pain state associated with that segment. In the next section, we describe the second classification layer of the proposed framework.

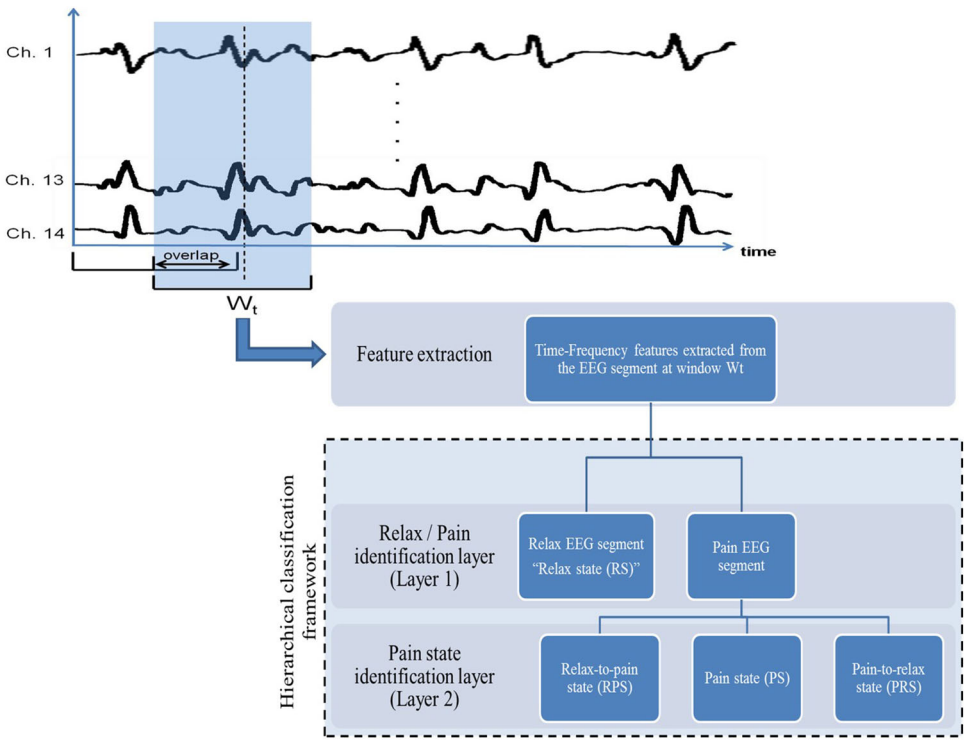

Fig. 2 An overall structure diagram of the proposed hierarchical classification framework. A sliding window is employed to decompose the signals of the 14 EEG channels ($Ch.1 - Ch.14$) into overlapping segments. Then, a set of nonlinear features are extracted and passed to the first classification layer, where the dimension of the extracted features depends on the employed evaluation procedure, as described in Sect. 2.6. The first layer identifies whether an EEG segment is a relax segment or a pain segment. In the second layer, the pain segments are classified into one of the three pain states (i.e., RPS, PS, and PRS)

2.5.2 The pain state identification layer (Layer 2)

In this layer, each EEG segment that is identified in layer 1 as pain segment is analyzed in order to determine the pain state associated with that segment. Specifically, we utilize the extracted nonlinear features to train a SVM classifier to identify whether a pain EEG segment belongs to the RPS, PS, or PRS, respectively. In this work, we employ a one-against-one scheme to implement a multi-class SVM classifier. Specifically, we construct three binary SVM classifiers, one for each pair of states.

In both classification layers, the performance of the SVM classifier with RBF kernel is highly dependent on the selected values for two different parameters: σ, the RBF kernel parameter, and $C > 0$, the regularization parameter. Therefore, in order to determine the parameters of the SVM classifier, we performed a grid-based search along two directions. In the first direction, we varied the value of the RBF kernel parameter σ, while in the second direction we varied the value of the parameter C. Then, the best SVM model is selected such that its parameters maximize the average classification accuracy.

2.6 Performance evaluation procedures and metrics

In this study, we evaluate the performance of the proposed approach using three different procedures:

1. *Wavelet-based performance evaluation procedure* In this procedure, we address the effect of selecting different wavelet functions on the accuracy of identifying different tonic cold pain states in the EEG signals. In particular, we implemented five different classification models, similar to the model described in Sect. 2.4.2, where each model utilizes the nonlinear features described in Sect. 2.5. Each of these five classification models employs a unique wavelet function for performing the DWT analysis to extract the nonlinear features. The employed wavelet functions include the db4, db5, db8, sym6, and coif5. Moreover, for each classification model, the features are extracted from all the EEG channels and all frequency bands. Then, we evaluate the performance of each classification layer associated with each classification model in terms of the capability of identifying the four tonic cold pain states using the different wavelet functions.
2. *Channel-based performance evaluation procedure* In this procedure, we investigate the association between the different tonic cold pain states and brain activities occurring in different regions of the brain, including the frontal, mid frontal, central, and temporal regions. Considering the EEG data acquisition system described in Sect. 2.3, we have 14 channels arranged according to the international 10–20 system. These 14 channels are grouped into seven pairs of symmetric channels including: AF3–AF4, F3–F4, F7–F8, FC5–

FC6, O1–O2, P7–P8, and T7–T8. For the purpose of this procedure, we have developed seven different classification models, where each model utilizes the nonlinear features extracted from exactly one pair of the seven available symmetric channels using all frequency bands. Then, we evaluate the performance of both the first and second layers associated with each classification model in terms of the capability of identifying the four tonic cold pain states using the different pairs of symmetric channels.

3. *Frequency band-based performance evaluation procedure* The purpose of this evaluation procedure is to explore the effect of different EEG frequency bands, including delta, theta, alpha, beta, and gamma, on the accuracy of identifying the four states associated with tonic cold pain. In particular, we have developed five different classification models, where each model utilizes the nonlinear features extracted from one of the five frequency bands using all EEG channels. Then, we evaluate the performance of both the first and second layers associated with each classification model in terms of the capability of identifying the four tonic cold pain states using the different EEG frequency bands.

In order to evaluate the performance of the classification models in the aforementioned evaluation procedures, we utilize a fivefold cross-validation (CV) procedure. Specifically, for each subject, 80% of the data across the trials are selected for training, and the remaining data are used for testing. This procedure is repeated five times until all EEG signals are included in the testing. The average testing accuracy, precision, specificity, sensitivity, and F-1 measure are computed as performance evaluation metrics over the five train-test repetitions. These metrics are defined as follows [6, 7]:

$$\text{Accuracy} = \frac{(\text{TP} + \text{TN})}{(\text{TP} + \text{TN} + \text{FP} + \text{FN})}, \tag{8}$$

$$\text{Precision} = \frac{TP}{(TP + FP)}, \tag{9}$$

$$\text{Specificity} = \frac{\text{TN}}{(\text{TN} + \text{FP})}, \tag{10}$$

$$\text{Sensitivity} = \frac{\text{TP}}{(\text{TP} + \text{FN})}, \tag{11}$$

$$F_1 = \frac{2\text{TP}}{(2\text{TP} + \text{FP} + \text{FN})}, \tag{12}$$

where TP is the number of true-positive cases, TN is the number of true-negative cases, FP is the number of false-positive cases, and FN is the number of false-negative cases.

3 Experimental results and discussion

In order to evaluate the performance of the proposed tonic cold pain recognition approach, we performed the three evaluation procedures, as described in Sect. 2.6, based on the acquired EEG signals using the Emotiv EPOC + Neuroheadset. In this section, we provide the results obtained using each of the aforementioned three evaluation procedures. The experimental results of each evaluation procedure represent the average values computed for the 24 subjects.

3.1 Results of the wavelet-based analysis

In this section, we evaluate the effect of utilizing different types of wavelet functions on the accuracy of identifying tonic cold pain states from the acquired EEG signals. Specifically, we utilized five different wavelet functions to extract the nonlinear features from all the EEG channels and the EEG frequency bands. Then, using each one of the wavelet functions, we compute the performance of our proposed two-layer classification framework. Table 2 shows the results of identifying the tonic cold pain states for each wavelet function using precision, specificity, sensitivity, and F1-measure as an evaluation metrics [7]. The best performance was obtained when the nonlinear features were extracted using the db4 wavelet function. Specifically, the relax/pain identification layer (Layer 1) discriminated the EEG segments with relax state from pain segments with an overall average precision, specificity, sensitivity, and F1-measure of 93.52, 93.35, 87.77, and 89.93%, respectively. In addition, the pain state identification layer (Layer 2) classified the pain segments obtained from the relax/pain identification layer into RPS, PS, and PRS with an overall average precision, specificity, sensitivity, and F1-measure of 90.06, 94.51, 85.05, and 86.88%, respectively.

Figure 3 shows the average recognition accuracy for each layer in the classification framework using different wavelet functions. The best accuracies of both the first and the second classification layers were achieved when db4 was used as a wavelet function. The average accuracy of the first layer was 93.13%, while the average accuracy of the second layer was 88.93%. The results in Table 2 show that the highest true-positive rate and true-negative rate can be achieved using db4. This in turn can reduce the false-positive rate and the misclassification rate at both classification layers in comparison with the other wavelet functions. Therefore, in the next sections, we utilize the wavelet function db4 to extract the nonlinear features from EEG signals.

Table 2 Results of identifying the tonic cold pain states at the relax/pain identification layer (Layer 1) and the pain state identification layer (Layer 2) of the classification framework based on using different wavelet functions

			Precision (%)	Specificity (%)	Sensitivity (%)	F1-measure (%)
db4	Layer 1	RS	94.03	93.07	77.86	84.59
		pain	93.01	93.63	97.68	95.27
	Layer 2	RPS	89.82	94.13	88.44	88.75
		PS	92.04	94.78	75.80	82.54
		PRS	88.31	94.63	90.90	89.36
db5	Layer 1	RS	88.70	92.38	72.49	77.86
		pain	92.27	88.59	97.12	94.57
	Layer 2	RPS	88.28	94.72	90.21	89.09
		PS	91.65	94.43	74.69	81.77
		PRS	89.20	94.19	90.29	89.57
db8	Layer 1	RS	94.33	92.05	74.44	82.39
		pain	91.93	93.94	97.44	94.54
	Layer 2	RPS	86.34	92.44	84.91	85.25
		PS	88.94	93.50	73.99	80.39
		PRS	87.79	94.56	90.32	88.86
sym6	Layer 1	RS	93.38	92.90	75.90	81.99
		pain	92.81	92.95	97.55	95.08
	Layer 2	RPS	90.37	93.81	89.26	89.67
		PS	91.11	95.15	77.03	82.99
		PRS	88.58	94.77	90.51	89.31
coif5	Layer 1	RS	93.14	90.80	67.00	75.31
		pain	90.65	92.44	97.21	93.78
	Layer 2	RPS	87.53	92.29	84.19	85.13
		PS	90.06	92.73	65.36	72.35
		PRS	84.83	93.69	89.76	86.79

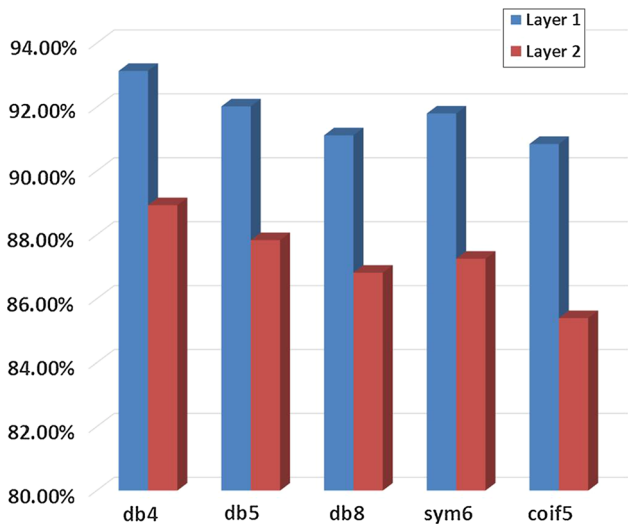

Fig. 3 Average accuracy of each layer in the classification framework using the five different wavelet functions

3.2 Results of the EEG channel-based analysis

In this section, we evaluate the effect of utilizing different symmetric pairs of EEG channels on the accuracy of identifying tonic cold pain states from the EEG signals. More specifically, the nonlinear features were extracted from seven different symmetric pairs of EEG channel, as described in Sect. 2.6. Then, using each one of the channel pairs, we compute the performance of our proposed two-layer classification framework. Table 3 shows the results of identifying the tonic cold pain states for each pair of symmetric channels using precision, specificity, sensitivity, and F1-measure as an evaluation metrics. The best performance was obtained when the nonlinear features were extracted from the pair F7–F8 in the frontal region of the brain using the db4 as a wavelet function. Specifically, the relax/pain identification layer (Layer 1) discriminated the EEG segments with relax state from the pain segments with an overall average precision, specificity, sensitivity, and F1-measure of 86.47, 86.43, 75.36, and 76.93%, respectively. In addition, the pain state identification layer (Layer 2) classified the pain segments obtained from the relax/pain identification layer into RPS, PS, and PRS with an overall average precision, specificity, sensitivity, and F1-measure of 84.88, 91.13, 72.45 and 73.83%, respectively. Figure 4 provides the average recognition accuracy for each layer in the classification framework using

Table 3 Results of identifying the tonic cold pain states at each layer in the proposed classification framework using different pairs of symmetric EEG channels

			Precision (%)	Specificity (%)	Sensitivity (%)	F1-measure (%)
AF3–AF4	Layer 1	RS	80.53	85.10	44.58	52.55
		pain	84.91	79.74	98.43	90.87
	Layer 2	RPS	80.39	90.19	78.73	75.76
		PS	71.49	89.53	42.69	47.97
		PRS	77.61	89.86	79.42	76.29
F3–F4	Layer 1	RS	90.61	85.45	44.91	53.46
		pain	85.30	89.94	98.50	91.28
	Layer 2	RPS	72.38	87.74	73.94	69.91
		PS	76.30	87.99	37.99	44.23
		PRS	74.41	84.44	73.76	71.12
F7–F8	Layer 1	RS	85.93	87.12	52.76	61.86
		pain	87.00	85.73	97.96	92.00
	Layer 2	RPS	84.56	90.22	80.72	79.83
		PS	88.09	91.40	54.90	62.17
		PRS	81.98	91.76	81.73	79.49
FC5–FC6	Layer 1	RS	73.62	82.94	33.03	38.98
		pain	82.78	73.31	97.78	89.49
	Layer 2	RPS	81.89	89.77	79.37	77.71
		PS	82.37	90.24	51.32	58.94
		PRS	81.02	91.32	81.51	79.22
O1–O2	Layer 1	RS	83.23	84.49	43.72	52.43
		pain	84.33	82.80	98.63	90.72
	Layer 2	RPS	80.87	90.24	79.75	78.93
		PS	93.49	89.97	52.23	61.07
		PRS	80.37	90.25	83.87	81.01
P7–P8	Layer 1	RS	90.57	85.83	46.60	56.55
		pain	85.62	90.56	98.74	91.60
	Layer 2	RPS	77.86	86.31	77.62	75.27
		PS	65.79	88.17	37.47	43.49
		PRS	75.70	88.44	77.53	74.44
T7–T8	Layer 1	RS	93.82	85.84	49.59	59.16
		pain	85.72	91.10	98.14	91.40
	Layer 2	RPS	76.49	88.19	71.31	68.47
		PS	76.74	88.41	40.18	48.46
		PRS	77.12	91.25	84.65	79.17

different pairs of symmetric EEG channels. The best accuracies of both the first and second classification layers were achieved using the F7–F8 channels. The average accuracy of the first layer was 87.73%, while the average accuracy of the second layer was 80.89%. Although the results in Table 3 show that the highest sensitivity and specificity is achieved using the pair F7–F8, the performance of the other pairs located at different brain regions is considered relatively close to the F7–F8 performance. The obtained results suggest that different brain regions, which have various functionalities, are involved during pain stimulation. This suggestion complies with the findings reported in [17]. The involvement of different brain regions during pain stimulation can be attributed to the fact that the frontal and the parietal regions in the brain are associated with emotional responses [2, 24] and processing sensory information related to the sense of touch [29], respectively.

3.3 Results of the EEG frequency band-based analysis

In this section, we evaluate the effect of utilizing different frequency bands of EEG signals on the accuracy of identifying tonic cold pain states based on the EEG

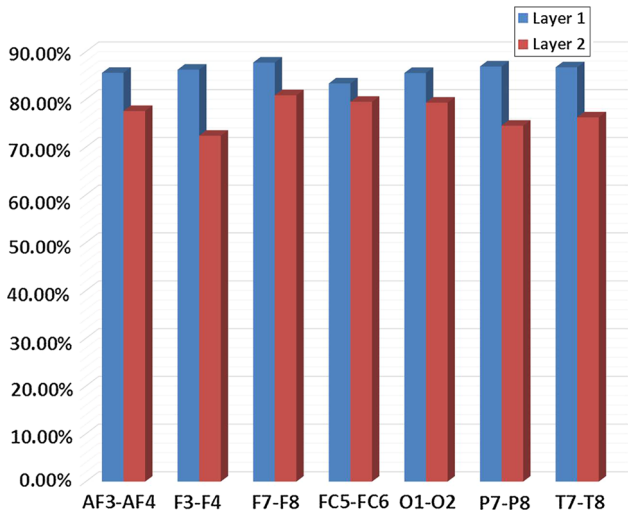

Fig. 4 Average accuracy of each layer in the classification framework using the seven different symmetrical pairs of EEG channels

signals. More specifically, the nonlinear features were extracted from five different frequency bands using all EEG channels, as described in Sect. 2.6. Then, using each frequency band, we compute the performance of our proposed two-layer classification framework. The obtained results for tonic cold pain states identification using precision, specificity, sensitivity, and F1-measure as an evaluation metrics are listed in Table 4. The best performance was obtained when the nonlinear features were extracted from the beta frequency band (13–30 HZ) using the db4 as a wavelet function. Specifically, the relax/pain identification layer (Layer 1) discriminated the EEG segments with relax state from pain segments with an overall average precision, specificity, sensitivity, and F1-measure of 94.02, 93.92, 88.88, and 90.58%, respectively. In addition, the pain state identification layer (Layer 2) classified the pain segments obtained from the relax/pain identification layer into RPS, PS, and PRS with an overall average precision, specificity, sensitivity, and F1-measure of 91.34, 95.10, 86.99, and 88.75%, respectively. Figure 5 shows the average recognition accuracy for each layer in the classification framework using different frequency bands. The best accuracies of both the first and the second classification layers were achieved using the beta frequency band. The average accuracy of the first layer was 93.86%, while the average accuracy of the second layer was 90.18%. These results are consistent with the findings reported in previous quantitative EEG studies, in which the EEG power in the frequency range (13–30 Hz) was found to increase significantly under tonic cold pain condition [14, 17, 33].

3.4 Comparison with other approaches

In this section, we compare the performance of the features proposed in this study, which are based on time–frequency analysis, with two frequency-based features that were introduced in [27] and [28]. Specifically, in the study presented in [27], the authors utilized the peak alpha frequency (PAF) as a frequency-based feature to characterize tonic heat pain in EEG signals. The PAF is defined as the frequency value at which the PSD has the highest value within the alpha frequency band (8–13 Hz). In order to compare the capability of our proposed wavelet-based features with the PAF feature in terms of the capability of characterizing the four different tonic cold pain states considered in our study, we have computed the PAF for the EEG signals in our tonic cold pain dataset and utilized these PAF values as features to construct our two-layered hierarchical classification framework. Table 5 provides the results of identifying the tonic cold pain states at the relax/pain identification layer (Layer 1) and the pain state identification layer (Layer 2) of the classification framework using the PAF features. To facilitate the comparison, we have also included the results obtained using our proposed wavelet-based features extracted from the D_3 DWT coefficients (alpha band) in Table 5. The results in Table 5 show that the average recognition accuracy of the first layer and the second layer obtained using the PAF features was 81.11 and 71.48%, respectively. On the other hand, the average accuracy of the first layer and the second layer obtained using our proposed wavelet-based features was 90.27 and 84.12%, respectively.

Similarly, in [28], the authors proposed the use of two frequency-based features, namely the normalized PSDs of the alpha frequency band (8–13 Hz) and the beta frequency band (13–30 Hz), to characterize the tonic heat pain in EEG signals. In order to compare the performance of the approach in [28] with our proposed approach, we computed the two features described in [28] for all the channels in the EEG signals in our tonic cold pain dataset. Then, using each one of these two features, we constructed our two-layered hierarchal classification framework to characterize the four different tonic cold pain states. Table 5 provides the results of identifying the tonic cold pain states at the relax/pain identification layer (Layer 1) and the pain state identification layer (Layer 2) of our classification framework using each of these two features. To facilitate the comparison, we have also included the results obtained using our proposed wavelet-based features extracted from the D_3 DWT coefficients (alpha band) and the D_2 DWT coefficients (beta band) in Table 5. The results in Table 5 show that the average recognition accuracies of the first layer and the second layer obtained using the normalized PSD in the alpha band feature were 83.11 and 71.48%,

Table 4 Results of identifying the tonic cold pain states at the relax/pain identification layer (Layer 1) and the pain state identification layer (Layer 2) of the classification framework using different EEG frequency bands

			Precision (%)	Specificity (%)	Sensitivity (%)	F1-measure (%)
Gamma	Layer 1	RS	89.84	86.80	52.15	61.84
		pain	86.60	89.51	97.20	91.51
	Layer 2	RPS	77.98	91.12	82.55	78.61
		PS	75.82	85.94	28.70	35.42
		PRS	78.36	90.69	81.03	77.81
Beta	Layer 1	RS	93.94	94.16	80.18	85.39
		pain	94.09	93.68	97.57	95.77
	Layer 2	RPS	90.44	94.59	89.97	90.03
		PS	93.16	95.48	79.53	85.45
		PRS	90.43	95.23	91.47	90.76
Alpha	Layer 1	RS	91.20	89.76	62.71	70.08
		pain	89.69	91.01	97.95	93.56
	Layer 2	RPS	85.87	91.96	83.00	82.91
		PS	88.49	92.41	59.30	67.87
		PRS	84.77	93.07	87.22	85.09
Theta	Layer 1	RS	82.40	84.22	38.39	46.70
		pain	83.19	82.67	98.66	90.05
	Layer 2	RPS	76.88	88.97	78.18	75.12
		PS	57.79	87.77	38.49	43.53
		PRS	79.31	90.52	79.20	74.74
Delta	Layer 1	RS	83.31	81.32	27.02	34.21
		pain	80.48	83.88	99.32	88.70
	Layer 2	RPS	72.56	87.25	72.78	67.47
		PS	46.47	86.21	23.66	27.01
		PRS	68.58	88.57	71.93	66.19

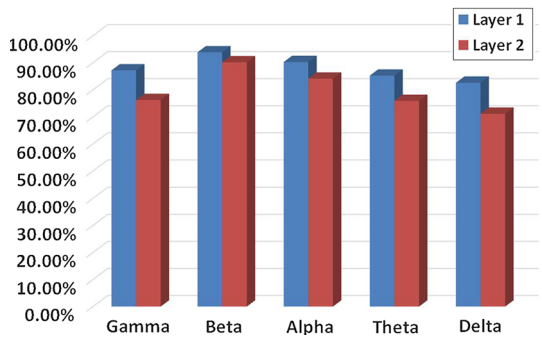

Fig. 5 Average accuracy of each layer in the classification framework using the five different frequency bands

respectively. On the other hand, the average accuracies of the first and the second layers achieved using our proposed wavelet-based features that were extracted from the alpha band were 90.27 and 84.12%, respectively. Similarly, the average recognition accuracy of the first layer and the second layer obtained using the normalized PSD in the beta band feature was 83.11 and 71.48%, respectively. In comparison, the average accuracies for the first and the second layers achieved using our proposed wavelet-based features that were extracted from the beta band were 90.27 and 84.12%, respectively. The experimental results presented in Table 5 demonstrate the efficacy of our proposed approach for accurate tonic cold pain identification compared with the other two features described in [27, 28].

4 Conclusion and future work

In this paper, a feasibility study has been presented to investigate the capability for detecting tonic cold pain based on EEG signals analysis. In particular, DWT was utilized to obtain a time–frequency representation of the EEG signals. Then, a set of nonlinear features were computed and used to train a two-layer hierarchical classification model. In the first layer, EEG segments were classified into relax or pain segments. In the second layer, each EEG segment that was identified in layer 1 as pain segment is analyzed in order to determine the pain state associated with that segment. Three different analysis procedures were conducted to quantify the effect of utilizing different wavelet functions, EEG channel pairs, and EEG frequency bands. These evaluation procedures were applied to the EEG signals obtained from 24 healthy subjects that were

Table 5 Comparison of classification performance obtained for various features presented in [27, 28] as well as the features proposed in the current study

Method	Features	Layer	Class	Precision (%)	Specificity (%)	Sensitivity (%)	F1 measure (%)	Layer's average accuracy (%)
Our approach	Eight nonlinear features extracted from the D_3 DWT coefficients (alpha band) using all EEG channels	Layer 1	no-pain	91.2	89.7	62.7	70.0	90.2
			Pain	89.6	91.0	97.9	93.5	
		Layer 2	RPS	85.8	91.9	83.0	82.9	84.1
			PS	88.4	92.4	59.3	67.8	
			PRS	84.7	93.0	87.2	85.0	
[27]	PAF extracted from the alpha band using all EEG channels	Layer 1	no-pain	78.7	82.37	34.8	44.3	81.1
			Pain	82.2	78.4	97.4	89.1	
		Layer 2	RPS	72.6	82.0	71.2	68.4	71.4
			PS	69.5	86.8	32.8	39.1	
			PRS	67.4	87.0	72.1	67.9	
[28]	Normalized PSD in alpha band using all EEG channels	Layer 1	no-pain	36.4	76.0	17.8	22.3	75.6
			Pain	75.9	36.2	94.0	83.7	
		Layer 2	RPS	60.4	71.3	70.1	62.4	61.7
			PS	23.0	82.5	13.5	13.9	
			PRS	52.2	74.5	57.9	51.6	
Our approach	Eight nonlinear features extracted from the D_2 DWT coefficients (beta band) using all EEG channels	Layer 1	no-pain	93.9	94.1	80.1	85.3	93.8
			Pain	94.0	93.6	97.5	95.7	
		Layer 2	RPS	90.4	94.5	89.9	90.0	90.1
			PS	93.1	95.4	79.5	85.4	
			PRS	90.4	95.2	91.4	90.7	
[28]	Normalized PSD in beta band using all EEG channels	Layer 1	no-pain	33.1	77.8	14.0	18.02	78.71
			Pain	77.7	32.5	99.4	87.0	
		Layer 2	RPS	54.2	63.2	55.4	48.6	57.7
			PS	23.9	82.4	11.7	12.0	
			PRS	47.6	69.5	60.8	51.2	

exposed to tonic cold pain stimulation. This stimulation leads to the following states: relax state, relax-to-pain state, pain state, and pain-to-relax state. The results of the wavelet analysis show that using the db4 as a wavelet function provides the best accuracies of both the first and the second classification layers, with average accuracies of 93.13 and 88.93%, respectively. Furthermore, the results of the EEG channel analysis suggest that different brain regions with various functionalities are involved during pain stimulation. Finally, the results of the EEG frequency band analysis show that the best accuracies of both the first and the second classification layers can be achieved using the beta band with average accuracies of 93.86 and 90.18%, respectively. The results reported in Sect. 3 demonstrate the feasibility of combining the wavelet-based features along with the two-layered SVM-based classification framework to achieve accurate identification of tonic cold pain states.

In the future, we intend to extend the proposed approach by employing different time–frequency representations, such as time–frequency distributions along with higher-order spectral-based features. Furthermore, we plan to expand our database to enable the study of the correlation between the extracted features and other emotional description scales, such as the valence and arousal scales. In addition, we plan to investigate the application of our approach to analyze clinical pain, such as cancer pain.

Acknowledgements This research is supported by the Seed Grant program at the German Jordanian University (Grant no. SAMS 8/2014), and partially supported by the Scientific Research Support Fund - Jordan (Grant no. ENG/1/9/2015).

Compliance of ethical standards

Conflict of Interest The authors declare that they have no conflict of interest.

References

1. Abibullaev B, Kim MS, Seo HD (2010) Seizure detection in temporal lobe epileptic EEGs using the best basis wavelet functions. J Med Syst 34(4):755–765
2. Aftanas L, Reva N, Varlamov A, Pavlov S, Makhnev V (2004) Analysis of evoked EEG synchronization and desynchronization in conditions of emotional activation in humans: temporal and topographic characteristics. Neurosci Behav Physiol 34(8):859–867
3. Akansu AN, Haddad RA (2001) Multiresolution signal decomposition: transforms, subbands, and wavelets. Academic Press, Cambridge
4. Akin M (2002) Comparison of wavelet transform and FFT methods in the analysis of EEG signals. J Med Syst 26(3):241–247
5. Alazrai R, Alwanni H, Baslan Y, Alnuman N, Daoud M (2017) EEG-based brain–computer interface for decoding motor imagery tasks within the same hand using Choi–Williams time–frequency distribution. Sensors 17(9):1937
6. Alazrai R, Momani M, Daoud M (2017) Fall detection for elderly from partially observed depth-map video sequences based on view-invariant human activity representation. Appl Sci 7(4):316
7. Alazrai R, Mowafi Y, Lee CG (2015) Anatomical-plane-based representation for human–human interactions analysis. Pattern Recognit 48(8):2346–2363
8. Chang CC, Lin CJ (2011) Libsvm: a library for support vector machines. ACM Trans Intell Syst Technol 2(3):1–27
9. Chen AC (1993) Human brain measures of clinical pain: a review i. Topographic mappings. Pain 54(2):115–132
10. Christine M, Matthew B, Roger C, Yvonne D, Craig H, Laurie H, Jahangir Malekiand Renee M (2008) Principles of analgesic use in the treatment of acute pain and cancer pain. American Pain Society, Glenview
11. Chua K, Chandran V, Rajendra Acharya U, Lim C (2009) Analysis of epileptic EEG signals using higher order spectra. J Med Eng Technol 33(1):42–50
12. Chua KC, Chandran V, Acharya UR, Lim CM (2011) Application of higher order spectra to identify epileptic EEG. J Med Syst 35(6):1563–1571
13. Delorme A, Makeig S (2004) Eeglab: an open source toolbox for analysis of single-trial EEG dynamics including independent component analysis. J Neurosci Methods 134(1):9–21
14. Dowman R, Rissacher D, Schuckers S (2008) Eeg indices of tonic pain-related activity in the somatosensory cortices. Clin Neurophysiol 119(5):1201–1212
15. Emotiv Systems Inc. San Francisco, C.: URL https://www.emotiv.com/
16. Gómez-Herrero G, De Clercq W, Anwar H, Kara O, Egiazarian K, Van Huffel S, Van Paesschen W (2006) Automatic removal of ocular artifacts in the eeg without an eog reference channel. In: Proceedings of the 7th IEEE nordic signal processing symposium, pp 130–133
17. Hadjileontiadis LJ (2015) Eeg-based tonic cold pain characterization using wavelet higher order spectral features. IEEE Trans Biomed Eng 62(8):1981–1991
18. Herr K, Coyne PJ, McCaffery M, Manworren R, Merkel S (2011) Pain assessment in the patient unable to self-report: position statement with clinical practice recommendations. Pain Manag Nurs 12(4):230–250
19. Ingvar M (1999) Pain and functional imaging. Philos Transe R Soc Lond B Biol Sci 354(1387):1347–1358
20. Kamdar MM (2010) Principles of analgesic use in the treatment of acute pain and cancer pain. J Palliat Med 13(2):217–218
21. Khokhar ZO, Xiao ZG, Menon C (2010) Surface emg pattern recognition for real-time control of a wrist exoskeleton. BioMed Eng OnLine 9(1):41
22. Lamothe M, Roy JS, Bouffard J, Gagné M, Bouyer LJ, Mercier C (2014) ffect of tonic pain on motor acquisition and retention while learning to reach in a force field. PLoS ONE 9(6):e99,159
23. Lawhern V, Hairston WD, McDowell K, Westerfield M, Robbins K (2012) Detection and classification of subject-generated artifacts in EEG signals using autoregressive models. J Neurosci Methods 208(2):181–189
24. Mohammadi Z, Frounchi J, Amiri M (2016) Wavelet-based emotion recognition system using EEG signal. Neural Comput Appl pp 1–6
25. Nicolas-Alonso LF, Gomez-Gil J (2012) Brain computer interfaces, a review. Sensors 12(2):1211–1279
26. Nikias CL, Mendel JM (1993) Signal processing with higher-order spectra. IEEE Sig Process Mag 10(3):10–37
27. Nir RR, Sinai A, Raz E, Sprecher E, Yarnitsky D (2010) Pain assessment by continuous eeg: association between subjective perception of tonic pain and peak frequency of alpha oscillations during stimulation and at rest. Brain Res 1344:77–86
28. Panavaranan P, Wongsawat Y (2013) Eeg-based pain estimation via fuzzy logic and polynomial kernel support vector machine. In: 6th Biomedical engineering international conference (BMEiCON), pp 1–4
29. Penfield W, Rasmussen T, Erickson T (1954) The cerebral cortex of man, a clinical study of localization of function. Am J Phys Med Rehabil 33(2):126
30. Press WH, Teukolsky SA, Vetterling WT, Flannery BP (2007) Numerical recipes 3rd edition: the art of scientific computing. Cambridge University Press, New York
31. Price DD (2000) Psychological and neural mechanisms of the affective dimension of pain. Science 288(5472):1769–1772
32. Rissacher D, Dowman R, Schuckers S (2007) Identifying frequency-domain features for an eeg-based pain measurement system. In: IEEE 33rd annual northeast bioengineering conference,, pp 114–115
33. Shao S, Shen K, Yu K, Wilder-Smith EP, Li X (2012) Frequency-domain eeg source analysis for acute tonic cold pain perception. Clin Neurophysiol 123(10):2042–2049
34. Sinke C, Schmidt K, Forkmann K, Bingel U (2015) Phasic and tonic pain differentially impact the interruptive function of pain. PLoS ONE 10(2):e0118,363
35. Stam CJ (2005) Nonlinear dynamical analysis of eeg and meg: review of an emerging field. Clin Neurophysiol 116(10):2266–2301
36. Subha DP, Joseph PK, Acharya UR, Lim CM (2010) Eeg signal analysis: a survey. J Med Syst 34(2):195–212
37. Treede RD, Kenshalo DR, Gracely RH, Jones AK (1999) The cortical representation of pain. Pain 79(2):105–111
38. Vatankhah M, Toliyat A (2016) Pain level measurement using discrete wavelet transform. Int J Eng Technol 8(5):380
39. Williamson A, Hoggart B (2005) Pain: a review of three commonly used pain rating scales. J Clin Nurs 14(7):798–804